Observability metric for the relative localization of AUVs based on range and depth measurements: theory and experiments

Filippo Arrichiello, Gianluca Antonelli, Antonio Pedro Aguiar, Antonio Pascoal

Abstract— **This paper addresses the problem of observability of the relative motion of two AUVs equipped with velocity and depth sensors, and inter-vehicle ranging devices. We start by exploiting nonlinear observability concepts to analyze, using observability rank conditions, some types of relative AUV motions. Because rank conditions only provide binary information regarding observability, we then derive a specific observability index (metric) and study its dependence on the types of relative motions executed by the vehicles. In particular, it is shown that the degradation of observability depends on the range and angle between the relative velocity and position vectors. The problem addressed bears affinity with that of single beacon localization. For this reason, the results derived are validated experimentally in a equivalent, single beacon navigation scenario.**

I. INTRODUCTION

The problem of Autonomous Underwater Vehicle (AUV) localization is of paramount importance in the execution of commercial and scientific operations at sea. For this reason, this topic has been the object of intensive research effort in recent years. As is well known, localization devices such as GPS are ineffective underwater due to the attenuation of electromagnetic radiation, and can therefore only be used when the vehicles come to the surface. For this reason, a large class of underwater localization systems relies strongly on the propagation of sound waves in water. In many of them, the core principle of operation is the measurement of the time of flight of an acoustic signal between an emitter and a receiver to obtain an estimate of the distance between the two. Among the acoustic positioning systems that are available commercially, Long, Short, and Ultra-Short Baseline have found widespread use. More recently, a different method for AUV positioning that uses a simple transponder(beacon)/transducer couple has come to the fore. With this set-up, the position of the AUV can be obtained by complementing on-board available motion data (e.g., inertial velocity measured with a Doppler unit) with information on the range between the AUV and a transponder moored at a known location. This concept can be extended to address the problem of relative positioning between two AUVs, which motivated the study undertaken in the present paper.

The increasing attention paid to the problem of absolute (single vehicle) or relative (inter-vehicle) localization using ranging sensors is patent in a number of papers recently available in the literature. Among them, [3] and [4] present a discrete-time localization approach that, at each sampling instant, enumerates possible solutions to the localization problem and selects the most appropriate by minimizing an appropriate cost function. A generalization of this approach, complemented with experimental tests with an autonomous surface vessel (equipped with GPS) and an underwater vehicle are presented in [8]. The work reported makes ample use of the Woods Hole Oceanographic Institution (WHOI) acoustic modem [24], configured as a range measuring device.

In [18], a Synthetic Long Base Line (SLBL) localization system that uses a single transponder and multiple range measurements taken by an AUV at different locations along its trajectory is presented. In [10], a navigation algorithm based on an extended Kalman filter is proposed and the analysis of the observability conditions for the linear time-varying system obtained by linearizing the nonlinear system about a nominal trajectory is performed. The work in [19] describes how both bandwidth constraints and latency can be addressed in a Kalman filter framework. The observability study of planar single beacon navigation for AUVs in the presence of ocean current is presented in the PhD thesis in [9]. In [23], a solution to the problem of estimating an underwater vehicle position in the presence of unknown ocean currents is presented; in the proposed approach, at each sampling instant, the relative position of the vehicle w.r.t an underwater transponder is firstly computed using a multilateration-based approach, and then a Kalman filter is used to refine both the position and the current velocity estimates. In a recent paper [6], an approach to deal with the distortions effects of the sound-ray propagation in order to get accurate range measurements is presented, and its application to multi-robot underwater relative localization is discussed.

Observability issues for the problem of single beacon localization of autonomous vehicles are addressed in [5]. In the adopted set-up, the vehicle is equipped with a standard Inertial Measurement Unit (IMU), and range measurements with respect to a single source are available in addition to angular velocity readings. A state augmentation technique is used to derive a linear time-varying system that mimics the dynamics of the nonlinear system. A study on the observability of both the linear time-varying and non linear systems is presented, and analytical properties that make the system observable are derived. As a case study, numerical simulations are done with a model of a quadrotor.

The PhD thesis of Hartsfield [12] gives a summary of the

F. Arrichiello and G. Antonelli are with the Department DAEIMI of the University of Cassino, via G. Di Biasio 43, 03043 Cassino (FR), Italy {f.arrichiello,antonelli}@unicas.it

P. Aguiar and A. Pascoal are with the Laboratory of Robotics and Systems in Engineering and Science (LARSyS), IST, Technical University of Lisbon, Av. Rovisco Pais 1, 1049-001, Lisbon, Portugal {pedro,antonio}@isr.ist.utl.pt

state of the art on single beacon localization. Observability properties are not studied formally, but the concept of unobservable movements is heuristically discussed, e.g. radial motion.

In [14] the authors analyze the observability of a Global Positioning System/Inertial Navigation System and study the relations among observability, observability measures, estimation error covariance, and the information matrix associated with the problem at hand. It is shown that the observability measures have direct connections with the singular value decomposition of a properly defined information matrix. In contrast to what happens with the error covariance, the measures are determined by the system model and independent of the initial error covariance.

In [17] two tools, the local unobservability index and the local estimation condition number are introduced to measure the degree of observability or unobservability of autonomous systems (that is, systems with no inputs). Both measures are defined based on the singular values of the local observability Gramian of a conveniently defined linear model derived from the original nonlinear system. In order to simplify the computations, the paper shows how to build an approximate, empirical local observabilty Gramian. Reference [16] exploits the use of dynamical optimization and associated computational methods to define and quantitatively measure the observability of a nonlinear system.

On a different yet related vein, the stochastic approach introduced in [7] exploits the concept of a informational correlation coefficient inherited from signal theory to study the degree of observability of a discrete-time, stochastically autonomous system. The Fisher Information Matrix is used in [15] as a tool to obtain binary information about the observability of a nonlinear mapping. The results point to the possibility of using the singular values of the matrix to define a measure of observability. In [21], the problem of finding optimal maneuvers for bearings-only tracking systems is addressed, and a solution based on the Fisher Information Matrix is proposed.

In this paper, motivated by the above circle of ideas, we address observability issues related to the general problem of relative positioning of two underwater vehicles equipped with velocity and depth sensors and inter-vehicle ranging devices. We extend the work reported in [1] and [2], which built on the results available in [22]. We derive a specific observability index (metric) and study its dependence on the types of motion imparted to the vehicles. In particular, it is shown that the degradation of observability depends on the range between vehicles and the angle between the relative velocity and position vectors. The problem addressed bears affinity with that of single beacon localization. For this reason, to bridge the gap between theory and practice and validate some of the conclusions obtained, field tests were done with an autonomous surface vehicle equipped with with an acoustic ranging device capable of measuring its distance to a moored underwater transponder. The paper describes the results of the experiments and discusses plans for future research.

II. Observability Study

A. System model

Let $\Sigma_I : \{O_I - \boldsymbol{X}_I \boldsymbol{Y}_I \boldsymbol{Z}_I\}$ be a inertial, earth-fixed, reference frame defined according to the North East Down (NED) convention and let $\Sigma_{v,i} : \{O_{v,i} - \boldsymbol{X}_{v,i}\boldsymbol{Y}_{v,i}\boldsymbol{Z}_{v,i}\}; i = 1, 2$ be a frame with its origin fixed in the i-th vehicle centroid and parallel to Σ_I (see Fig. 1). In what follows, $\boldsymbol{x}_{v,1} \in \mathbb{R}^3$ and $\boldsymbol{x}_{v,2} \in \mathbb{R}^3$ denote the positions of the two vehicles with respect to Σ_I. Let $\boldsymbol{v}_{v,1} = d\boldsymbol{x}_{v,1}/dt$ and $\boldsymbol{v}_{v,2} = d\boldsymbol{x}_{v,2}/dt$ be the inertial velocities of vehicles 1 and 2, respectively and define their relative velocity as $\boldsymbol{v} = \boldsymbol{v}_{v,2} - \boldsymbol{v}_{v,1}$. Further, define the state $\boldsymbol{x} = \boldsymbol{x}_{v,2} - \boldsymbol{x}_{v,1}$. Assume it is possible to measure the distance between the vehicles as well as their velocities and depths. With this notation, a first order kinematic model that captures the relative motion of the vehicle is simply given by

$$\begin{cases} \dot{\boldsymbol{x}} = & \boldsymbol{v} \\ \boldsymbol{y} = & \begin{bmatrix} \frac{1}{2}\boldsymbol{x}^{\mathrm{T}}\boldsymbol{x} \\ x_3 \end{bmatrix} \end{cases} \tag{1}$$

where $\boldsymbol{x}$ is the state, $\boldsymbol{v}$ is the input, and $\boldsymbol{y}$ is the measurable output vector consisting of the distance between the two vehicles and their depth difference x_3.

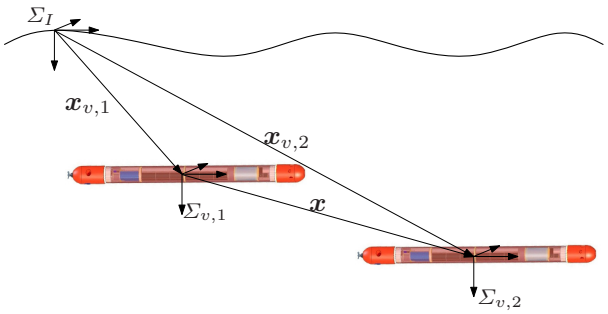

Fig. 1. Reference systems.

In the literature, the range-based localization problem is normally studied in 2D. Here, we include explicitly a third dimension (depth) to fully capture maneuvers that include diving. Notice also that because the above model is defined in terms of relative motion, it captures the kinematics of both single beacon as well as relative vehicle localization.

B. Observability of nonlinear systems

The concept of *local weak observability* was introduced by Hermann and Krener in [13] and discussed, e.g., in [20], for the general class of continuous-time, nonlinear dynamic systems described by

$$\begin{cases} \dot{\boldsymbol{x}} = & \boldsymbol{f}(\boldsymbol{x}, \boldsymbol{u}) \\ \boldsymbol{y} = & \boldsymbol{h}(\boldsymbol{x}) \end{cases}, \tag{2}$$

where $\boldsymbol{x} \in \mathbb{R}^n$, $\boldsymbol{u} \in \mathbb{R}^p$, and $\boldsymbol{y} \in \mathbb{R}^m$ are the state, input, and output respectively, $\boldsymbol{f}$ is the state vector field, and $\boldsymbol{h}$ is the output measurement equation. For an abridged overview of the important concepts of observability, Lie derivatives

and observability rank condition, the reader may wish to consult the presentation in [25] in the context of relative localization.

Define the Lie derivatives of the scalar output h_j as

$$\begin{aligned} \mathcal{L}_f^0 h_j &= h_j \\ \mathcal{L}_f^1 h_j &= \nabla h_j \cdot \boldsymbol{f} = \frac{\partial h_j}{\partial \boldsymbol{x}} \cdot \boldsymbol{f} = \sum_{i=1}^{3} \frac{\partial h_j}{\partial x_i} \cdot f_i \\ \mathcal{L}_f^2 h_j &= \frac{\partial}{\partial \boldsymbol{x}} \left[\mathcal{L}_f^1 h_j\right] \cdot \boldsymbol{f} \\ &\cdots \\ \mathcal{L}_f^n h_j &= \frac{\partial}{\partial \boldsymbol{x}} \left[\mathcal{L}_f^{n-1} h_j\right] \cdot \boldsymbol{f} \end{aligned} \tag{3}$$

where ∇ denotes the gradient operator. An important result on observability is given by the observability rank condition [13], [20, th. 3.32, p. 95], that states that the system (2) above is *locally weak observable* at state $x_o \in \mathbb{R}^n$ if the matrix

$$\mathcal{O} = \begin{bmatrix} \nabla \mathcal{L}_f^0 h_j \\ \nabla \mathcal{L}_f^1 h_j \\ \vdots \\ \nabla \mathcal{L}_f^k h_j \end{bmatrix}, \tag{4}$$

computed at x_o, is full rank for some index $k \in \mathbb{N}$; in the above, $\mathcal{L}_f^\alpha h_j$ is the set of the α-order Lie derivatives for any $j \in \{1, \ldots, m\}$.

C. Observability and metric of observability

For the system (1) it is possible to verify that it is always possible to select a velocity input v that allows satisfaction of the observability rank condition for all $\boldsymbol{x} \in \mathbb{R}^3$. In particular, it is easy to verify that system (1) is characterized by null $\nabla \mathcal{L}_f^1 h_2$ and null gradients of k-order Lie derivatives for $k \geq 2$. Since full rank of matrix $\mathcal{O}$ implies local weak observability and only a finite (and small) number of row are different from zero, it is appropriate to exploit the possibility of building a candidate observability submatrix $\overline{\boldsymbol{O}}$ obtained from $\mathcal{O}$ by keeping the 3 first rows. This yields

$$\overline{\boldsymbol{O}} = \begin{bmatrix} \nabla \mathcal{L}_f^0 h_1 \\ \nabla \mathcal{L}_f^0 h_2 \\ \nabla \mathcal{L}_f^1 h_1 \end{bmatrix} = \begin{bmatrix} \boldsymbol{x}^{\mathrm{T}} \\ \begin{bmatrix} 0 & 0 & 1 \end{bmatrix} \\ \boldsymbol{v}^{\mathrm{T}} \end{bmatrix} = \begin{bmatrix} x_1 & x_2 & x_3 \\ 0 & 0 & 1 \\ v_1 & v_2 & v_3 \end{bmatrix}, \tag{5}$$

where the notation $\boldsymbol{x} = [x_1, x_2, x_3]^T$ and $\boldsymbol{v} = [v_1, v_2, v_3]^T$ was used.

Notice that the above matrix is singular when

$$x_1 v_2 = x_2 v_1, \tag{6}$$

that is, when the projections of the relative position and velocity vectors $\boldsymbol{x}$ and $\boldsymbol{v}$, respectively in the horizontal plane are parallel.

It is important to notice that failure of the observability rank condition at a point does not necessarily imply local unobservability [20]. This statement is supported by our findings concerning what we later define as *radial movement*, i.e., for the case where relative position and velocity in the horizontal plane are aligned. Nevertheless, we propose to consider the numerical balance of the matrix involved in the observability rank condition as a metric for observability.

As expected, the vertical component of the state, being directly measured, does not influence the observability rank. A null determinant implies a singular matrix; however, it is important to bear in mind that the determinant of a matrix does not give a good measure of how close that matrix is to being singular. In fact, the distance of a matrix to the closest singular matrix (as evaluated by the Euclidean-induced matrix norm) is given by its minimum singular value [11, p. 82].

In the following we neglect the vertical components that is given by the depth measurements, and we study the 2D problem obtained by projecting all the vectors in the horizontal plane. With an obvious abuse of notation, we write the resulting equations as

$$\begin{cases} \dot{\boldsymbol{x}} &= \boldsymbol{v} \\ y &= \frac{1}{2} \boldsymbol{x}^{\mathrm{T}} \boldsymbol{x} \end{cases} \tag{7}$$

where $\boldsymbol{x}, \boldsymbol{v} \in \mathbb{R}^2$ contain the first two components of the vectors defined in (1). The matrix $\overline{\boldsymbol{O}} \in \mathbb{R}^{2\times 2}$ becomes

$$\overline{\boldsymbol{O}} = \begin{bmatrix} \boldsymbol{x}^{\mathrm{T}} \\ \boldsymbol{v}^{\mathrm{T}} \end{bmatrix}, \tag{8}$$

and its determinant is still null for $x_1 v_2 = x_2 v_1$. To study the numerical characteristic of the matrix, it is useful to represent the relative position and velocity vectors in polar coordinates as follows:

$$\begin{aligned} \boldsymbol{x} &= x \begin{bmatrix} \cos\alpha & \sin\alpha \end{bmatrix}^{\mathrm{T}} \\ \boldsymbol{v} &= v \begin{bmatrix} \cos\phi & \sin\phi \end{bmatrix}^{\mathrm{T}}. \end{aligned}$$

Let $\theta = \phi - \alpha$, i.e., the vectors are parallel when $\theta = 0$. By further defining

$$\gamma = \frac{x}{v} \tag{9}$$

it follows that

$$\overline{\boldsymbol{O}} = v \begin{bmatrix} \gamma\cos\alpha & \gamma\sin\alpha \\ \cos\phi & \sin\phi \end{bmatrix}. \tag{10}$$

From the above, the condition number $C \geq 1$ of $\overline{\boldsymbol{O}}$ is obtained as

$$C = \frac{\max\{\sigma_{1,2}\}}{\min\{\sigma_{1,2}\}} = \frac{\gamma^2 + 1 + \sqrt{\gamma^4 + 2\gamma^2\cos(2\theta) + 1}}{2\gamma\,|\sin(\theta)|} \tag{11}$$

where $\sigma_{1,2}$ are the two singular values of $\overline{\boldsymbol{O}}$ which, defined as functions of γ and θ, are given by

$$\sigma_{1,2} = v\frac{\sqrt{2}}{2}\sqrt{\gamma^2 + 1 \pm \sqrt{\gamma^4 + 2\gamma^2\cos(2\theta) + 1}}. \tag{12}$$

The condition number gives information about how well the matrix $\overline{\boldsymbol{O}}$ is conditioned (the matrix is well conditioned when C is close to 1). Figure 2 shows the inverse of the condition number C^{-1} as a function of γ and θ.

It is interesting to notice that C^{-1} has a maximum for

$$\begin{cases} \gamma &= 1 \quad \text{(i.e., } x = v\text{)} \\ \theta &= \pm\frac{\pi}{2} \end{cases} \tag{13}$$

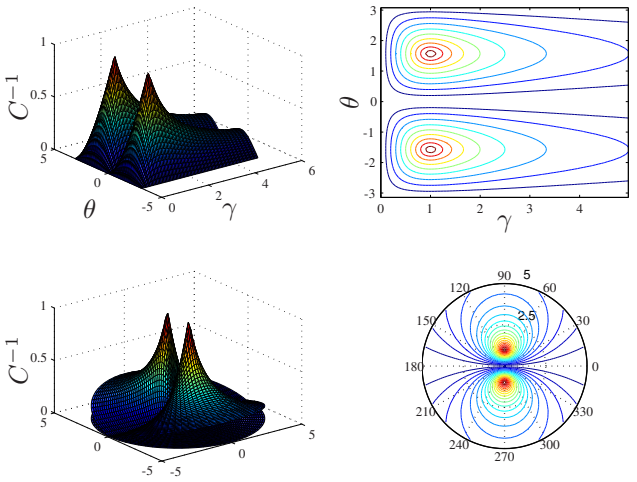

Fig. 2. Different views of the inverse of the condition number w.r.t θ (in radians) and k in Cartesian (top) and Polar (bottom) coordinates. The variable θ is the angle between relative velocity and position vectors, while the parameter k is the ration between their norms.

which corresponds to the situation where the relative position and velocity vectors are orthogonal and have the same magnitude. Notice also that C^{-1} is null for $\theta = 0$, or $\gamma = 0$, or $\gamma \to \infty$, the latter condition being observed when the ratio between the norms of $\boldsymbol{v}$ and $\boldsymbol{x}$ grows unbounded. The *optimum* condition (maximum of C^{-1}) can also be derived by noticing that, for a fixed γ, the determinant of $\overline{\boldsymbol{O}}$ has a maximum for $\theta = \pm\pi/2$. This follows from

$$\frac{\partial}{\partial\theta}\det(\overline{\boldsymbol{O}}) = 0 \quad \Rightarrow \frac{\cos\theta}{\gamma} = 0 \tag{14}$$

which corresponds to $\theta = \pm\pi/2$.

The following table shows how the ratio between x and v, defined as the parameter γ, plays an important role as a metric to assess the quality of observability.

	minimum sing. value	condition number
$\theta = 0$	0	∞
$\theta = \pm\pi/2$	$\min\{x, v\}$	$\max\{\frac{x}{v}, \frac{v}{x}\}$

An interesting observation that can be done by analyzing the proposed metric is that, assuming a constant relative speed, the observability conditions and therefore the expected performance of any position observer degrade when the distance between two AUVs (or between an AUV and a transponder in the case of single beacon localization) increases. This fact has been experimentally acknowledged by several researches (see e.g. [18]) but not formally proven. Notice also that the computation of the index given by the condition number of $\overline{\boldsymbol{O}}$ requires knowledge of x, v and θ; while the first two are actually available to the vehicle, the angle θ can not be measured/imposed if the AUV does not exactly know $\boldsymbol{x}$. Thus, to use the index for on-line path planning, θ can be imposed w.r.t the only currently estimated relative position.

In addition to what is presented in this paper, the *sensitivity* of the radial movement was also symbolically and numerically verified by resorting to the tools given in [17]. Finally, using a linearization approach or working with distances instead of the squares of distances yield results coherent with those presented in this paper; the discussion is omitted due to space limitations.

III. Experimental tests

In order to validate the results, field tests were planned and executed using an Autonomous Surface Vehicle (ASV) equipped with an acoustic modem and a GPS, while the second *vehicle* was actually an acoustic transponder fixed in a known position on the sea floor. The goal of the ASV was to estimate the transponder position by measuring its own velocity by resorting to the GPS, the transponder depth, and the relative range measured by the time of flight of the acoustic message exchange between the ASV and the transponder. The tests where performed in November 2010 at the Expo Area of Lisbon, Portugal (Lat: 38.766 Long: -9.03).

A. Experimental set-up

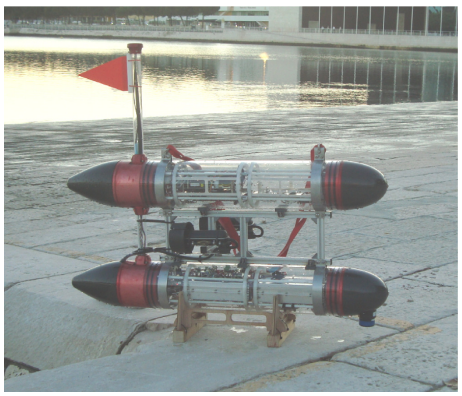

Fig. 3. The Medusa autonomous surface vessel

The ASV used in the experiments, named Medusa, was developed at the Laboratory of Robotics and Systems in Engineering and Science (LARSyS) of the Instituto Superior Técnico of Lisbon (see Fig. 3). The vehicle has two side thrusters that can be independently controlled to yield motions in surge and yaw. The vehicle is equipped with an IMU, a GPS, and a compass, and it can communicate with other devices via wifi or an underwater acoustic modem (Tritech Micron Modem, see Fig. 4-right). The transponder, installed at a known position underwater at 2 m depth, is essentially a Tritech Modem unit (Fig. 4-left) configured to respond to queries from the surface modem. Upon receiving a reply, the latter computes the round-trip travel time between the surface and the underwater units and, by knowing the speed of sound in the water measured before the tests, it estimates the corresponding distance. For powering and debugging purposes, the transponder was connected via a cable to a surface support system that was properly moored.

Fig. 4. Fixed transponder (left) and acoustic modem on the Medusa nose cone (right).

In each of the tests, the ASV was commanded to perform different paths specifically designed for the observability study: a set of parallel/orthogonal segments (some of which radial w.r.t the transponder) or circular paths (centered at the transponder). The stored data were post-processed to test the performance of an extended Luenberger observer. The filter was designed ready to be implemented on-board an autonomous marine robot and to take explicitly into account the low update frequency of the range measurement (one sample every few seconds) or even in the absence of the range signal: when no range information is available, the observer is updated by considering only the velocity measurement (a standard dead-reckoning approach).

Referring to eq. (2), the basic filter equation is of the form:

$$\dot{\hat{\boldsymbol{x}}} = \boldsymbol{f}(\hat{\boldsymbol{x}}, \boldsymbol{u}) + \boldsymbol{K}\left(\boldsymbol{y} - \boldsymbol{h}(\hat{\boldsymbol{x}})\right) \tag{15}$$

where $\boldsymbol{K}$ is a proper filter gain matrix.

We do not provide further details about the filter used because it is a standard solution and filtering is not the main contribution of this paper; in fact, the emphasis is on the evaluation of the filter performance by taking into account the observability metric adopted.

B. Experimental results

Several tests were run and the data were processed, leading to coherent results among them. Due to space constraints, only one case study is reported here. A video with additional case studies can be downloaded from `http://webuser.unicas.it/lai/robotica/video.html`.

The ASV is commanded to follow a set of parallel and orthogonal segments in an area of about 100m$\times$100m. Figure 5 shows the path of the ASV during the mission. In the background it is worth noticing the Transponder position (marked with the blue star), and the remote base station (Medusa Base) in charge of receiving and storing data from the ASV; the black squares represent the estimated position of the transponder during different mission steps.

Figure 6 shows the main data concerning the observability study. The top plot shows the inverse of the condition of the observability matrix of eq. (8) computed considering both real (in blue) and estimated (in green) relative displacement. As a ground truth data, the real displacement $\boldsymbol{x}$ is obtained using GPS readings of the ASV and the exact positioning of the transponder; the estimated displacement $\hat{\boldsymbol{x}}$ is given by the extended Luenberger observer. The second plot of Fig. 6 shows the estimation error of the observer. The filter

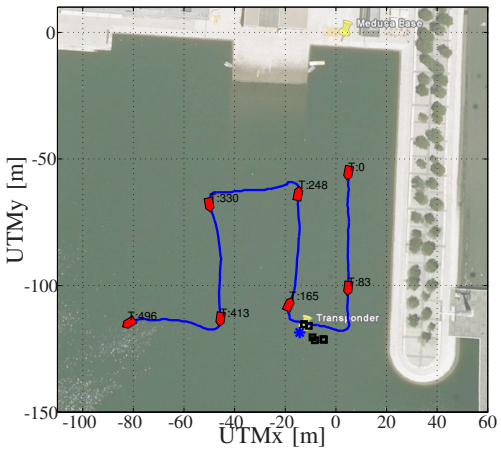

Fig. 5. Path of the robot during the case study.

is initialized so that the initial estimated position of the transponder is on a circle centered at the ASV and with radius equal to the range measurement, at a distance of 10m from the real transponder position. The third plot of Fig. 6 shows the range measured with the acoustic modem (in blue) and obtained from GPS data (in red). It is important to notice that the modem measurement is quite accurate but the update frequency is slow and there are some time windows with temporary communication losses (which is expected, in view of the adverse conditions of acoustic propagation in extremely shallow waters). The last plots of Fig. 6 respectively show the values of k, $\sin(\theta)$, and $\cos(2\theta)$ (referring to eq. (11)).

At this point, it is important to identify in Figs. 5 and 6 some noteworthy mission segments. Notice that when the ASV is moving closer to the transponder (during the [80s 180s] time window) the filter error decreases faster than when the vehicle is far from it. Notice also that when no range measurements are available the filter error is kept low using dead-reckoning data. Finally, Fig. 7 shows the linear velocity and heading of the ASV (computed using a GPS and IMU/compass data) while the multimedia attachment shows an animation of the ASV motion and the filter dynamics.

IV. Conclusion

The paper addressed observability issues in the context of the relative localization of autonomous underwater vehicles. By exploiting nonlinear observability concepts, a specific metric was proposed to study how the observability depends on the relative vehicle motions. Experimental results validate the considerations done. Future research will address the study of other types of observers, optimal real-time trajectory planning and multiple vehicle observability issues.

Acknowledgments

The research leading to these results has received funding from the European Community's Seventh Framework Programme under grant agreement n. 231378 (STREP project Co^{3}AUVs), the Italian Government, under Grant FIRB - Futuro in ricerca 2008 n. RBFR08QWUV (NECTAR project), and Portuguese project CONAV/FCT-PT (PTDC/EEA-CRO/113820/2009)

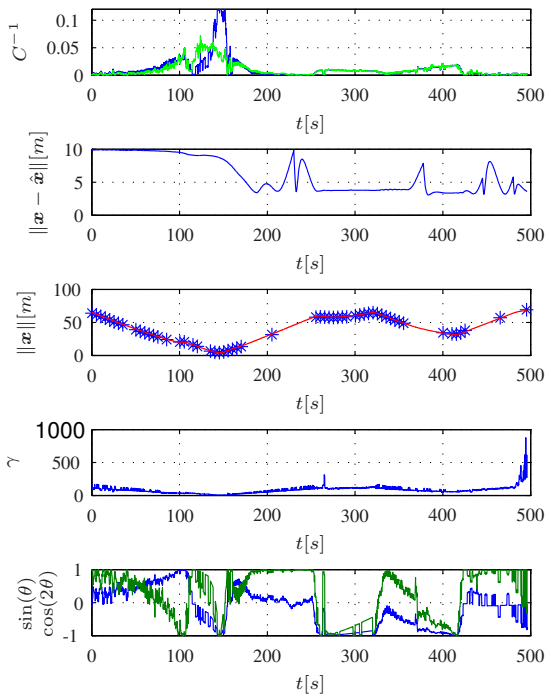

Fig. 6. Observability parameters during the first mission: inverse of condition number (top plot) calculated using real (blue) or estimated (green) positioning, filtering error (second plot from top), distance measured via modem and GPS (third plot), k (fourth plot) and $\sin(\theta)$ (blue) and $\cos(2\theta)$ (green) (last plot).

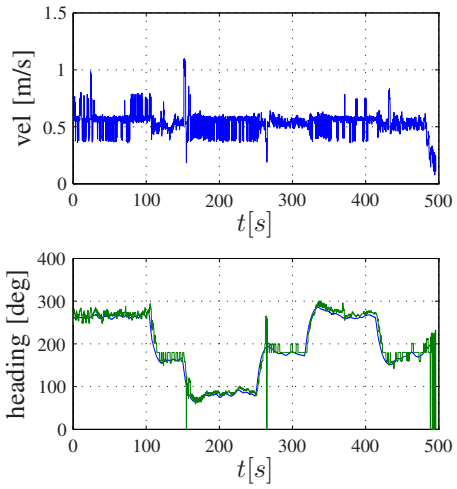

Fig. 7. Linear velocity and heading measured using GPS and IMU during the first mission.

REFERENCES

[1] G. Antonelli, F. Arrichiello, S. Chiaverini, and G.S. Sukhatme. Observability analysis of relative localization for AUVs based on ranging and depth measurements. In *Proceedings 2010 IEEE International Conference on Robotics and Automation*, pages 4276–4281, Anchorage, USA, May 2010.

[2] G. Antonelli, A. Caiti, V. Calabrò, and S. Chiaverini. Designing behaviors to improve observability for relative localization of AUVs. In *Proceedings 2010 IEEE International Conference on Robotics and Automation*, pages 4270–4275, Anchorage, AK, May 2010.

[3] A. Bahr. *Cooperative localization for autonomous underwater vehicles*. PhD thesis, Massachusetts Institute of Technology & Woods Hole Oceanographic Institution, 2008.

[4] A. Bahr, J.J. Leonard, and M.F. Fallon. Cooperative localization for autonomous underwater vehicles. *The International Journal Robotics Research*, 28:714–728, June 2009.

[5] P. Batista, C. Silvestre, and P. Oliveira. Single beacon navigation: observability analysis and filter design. In *Proceedings 2010 American Control Conference*, pages 6191–6196, Baltimore, MD, June 2010.

[6] G. Casalino, A. Caiti, A. Turetta, and E. Simetti. RT^2: real-time ray-tracing for underwater range evaluation. *Intelligent Service Robotics*, pages 1–12, 2011. 10.1007/s11370-011-0093-8.

[7] B. Chen, J. Hu, H. Li, and Z. Sun. Measure observability by the generalized informational correlation. In *46th IEEE Conference on Decision and Control*, pages 5570–5574, New Orleans, LA, December 2007.

[8] M.F. Fallon, G. Papadopoulos, J.J. Leonard, and N.M. Patrikalakis. Cooperative AUV navigation using a single maneuvering surface craft. *The International Journal of Robotics Research*, 29(12):1461–1474, 2010.

[9] A. Gadre. *Observability analysis in navigation systems with an underwater vehicle application*. PhD thesis, 2007.

[10] A.S. Gadre and D.J. Stilwell. Underwater navigation in the presence of unknown currents based on range measurements from a single location. In *Proceedings 2005 American Control Conference*, pages 565–661, Portland, OR, June 2005.

[11] G.H. Golub and C.F. Van Loan. *Matrix Computations*. The Johns Hopkins University Press, Baltimore, MD, third edition, 1996.

[12] J.C. Hartsfield. *Single transponder range only navigation geometry (STRONG) applied to REMUS autonomous underwater vehicles*. PhD thesis, 2005.

[13] R. Hermann and A. Krener. Nonlinear controllability and observability. *IEEE Transactions on Automatic Control*, 22(5):728–740, 1977.

[14] S. Hong, H.H. Chun, S.H. Kwon, and M.H. Lee. Observability measures and their application to GPS/INS. *Vehicular Technology, IEEE Transactions on*, 57(1):97–106, 2008.

[15] C. Jauffret. Observability and Fisher information matrix in nonlinear regression. *IEEE Transactions on Aerospace and Electronic Systems*, 43(2):756–759, 2007.

[16] W. Kang and L. Xu. A quantitative measure of observability and controllability. In *48th IEEE Conference on Decision and Control and 28th Chinese Control Conference*, pages 6413–6418, Shanghai, PRC, December 2009.

[17] A.J. Krener and K. Ide. Measures of unobservability. In *48th IEEE Conference on Decision and Control and 28th Chinese Control Conference*, pages 6401–6406, Shanghai, PRC, December 2009.

[18] M.B. Larsen. Synthetic long baseline navigation of underwater vehicles. In *Proceedings MTS/IEEE Conference Oceans 2000*, pages 2043–2050, 2000.

[19] D.K. Maczka, A.S. Gadre, and D.J. Stilwell. Implementation of a cooperative navigation algorithm on a platoon of autonomous underwater vehicles. In *Proceedings MTS/IEEE Conference Oceans 2000*, pages 1–6, 2007.

[20] H. Nijmeijer and A.J. Van der Schaft. *Nonlinear dynamical control systems*. Springer, 1990.

[21] J.M. Passerieux and D. Van Cappel. Optimal observer maneuver for bearings-only tracking. *Aerospace and Electronic Systems, IEEE Transactions on*, 34(3):777–788, July 1998.

[22] S. Roumeliotis and G. Bekey. Distributed multirobot localization. *IEEE Transactions on Robotics and Automation*, 18(5):781–795, 2002.

[23] J. Saúde and A.P. Aguiar. Single beacon acoustic navigation for an AUV in the presence of unknown ocean currents. In *Proceedings 8th IFAC Conference on Manoeuvring and Control of Marine Craft*, pages 298–303, Guarujá, BR, September 2009.

[24] S. Singh, M. Grund, B. Bingham, R. Eustice, H. Singh, and L. Freitag. Underwater acoustic navigation with the WHOI micro-modem. In *Proceedings MTS/IEEE Conference and Exhibition OCEANS 2000*, 2000.

[25] X.S. Zhou and S.I. Roumeliotis. Robot-to-robot relative pose estimation from range measurements. *IEEE Transactions on Robotics*, 24(6):1379–1393, Dec. 2008.